Supporting Information

Wu et al. 10.1073/pnas.0905670107

SI Text

SI Materials and Methods. ***Sample preparation and plasmid construction.*** The mCherry pRSET B plasmid was a kind gift from Dr. R. Y. Tsien (University of California, San Diego). mCherry was amplified by polymerase chain reaction (PCR) with a 5′ primer that encodes an NheI restriction site and a 3′ primer that encodes an *Xho*I site. The PCR fragment of mCherry was ligated into the backbone of pEGFP-C1 (Clonetech) to generate the mCherry-C1 vector for mammalian expression. For the sake of brevity, we refer to EGFP as G and to mCherry as Ch when naming protein constructs. The PCR fragments of mouse retinoid X receptor (RXRα) and human transcription intermediate factor 2 (TIF-2) were inserted into the mCherry-C1 or pEGFP-C1 vector at *Xho*I and *Eco*RI sites to construct Ch-RXR and G-TIF-2. The ligand binding domain of RXR from mouse (mRXRβ) was inserted into the mCherry-C1 plasmid at the *Xho*I and *Eco*RI sites to construct Ch-RXRLBD.

CV-1 cells were obtained from American Type Culture Collection and maintained in 10% fetal bovine serum (Invitrogen) and Dulbecco-modified Eagle's medium (Biowhittaker). Cells were subcultured into eight-well coverglass chamber slides (Nalge Nunc International) and then transiently transfected using transfectin (Bio-Rad) according to the manufacturer's instructions. Before conducting measurements, the growth media was removed and replaced with Leibovitz L15 (Invitrogen). All measurements were performed in the cell nucleus.

The activation of RXR is performed with RXR specific ligand 9-*cis* retinoic acid (Sigma-Aldrich Corporation) at a concentration of 1 μM.

Immunoblot analysis. Transfected CV-1 cells in six-well plates were directly lysed with 150 μL lysis buffer [100 mM Tris-HCl, pH 7.4; 1% Triton X-100; 5 mM EDTA; Protease inhibitor cock tail tablet (Roche)] 24 h after transfection, subjected to sodium dodecyl sulphate–polyacrylamide gel electrophoresis (Nupage Novex 4–12% Bis-Tris Gel in MOPS buffer; Invitrogen) and blotted on Hybond-ECL membrane (Amersham Biosciences). Immunodetection of target proteins was carried out with the following primary antibodies: mouse monoclonal anti-GFP (Roche), rabbit polyclonal anti-DsRed (Clonetech), mouse monoclonal anti-Tif-2 (BD Biosciences) antibodies. The anti-DsRed antibody is used to identify mCherry-labeled proteins. Detection was performed by visualization with IRDye 800 labeled anti-rabbit or Alexa 680 labeled anti-mouse secondary antibodies (Odyssey infrared imaging system; LI-COR Inc.). Quantification of Western blots was done using ImageJ (National Institutes of Health).

Brightness calibration and heterospecies partition (HSP) analysis. The brightness of EGFP and mCherry are determined by independent measurements of cells expressing each protein alone. The factorial cumulants of the photon counts are fit with time-integrated fluorescence cumulant analysis [TIFCA (1, 2)] to a single-species model, which determines the brightness $\vec{\lambda}_D = (\lambda_{\mathbf{G},D}, \lambda_{\mathbf{R},D})$ of EGFP and the brightness $\vec{\lambda}_A = (\lambda_{\mathbf{G},A}, \lambda_{\mathbf{R},A})$ of mCherry. The choice of subscripts (D = EGFP and A = mCherry) is motivated by EGFP being the donor and mCherry the acceptor, if Förster resonance energy transfer (FRET) is present. The brightness values of EGFP and mCherry serve as a calibration and are used to predict the brightness of the heterocomplex DA_n as described in ref. 3.

Fluorescence fluctuation spectroscopy (FFS) experiments on interacting proteins labeled with EGFP and mCherry are analyzed by TIFCA using the HSP model. This model fits the data to a two-species model with the constraint that the brightness of one of the species vanishes in the red channel. The fit parameters of the other species characterize the heterospecies as described in the main text.

Determining cellular protein concentrations and expression ratios. The total protein concentration and the concentration ratio between mCherry labeled protein $[A]$ and EGFP labeled protein $[D]$ are identified from fluorescence intensity measurements. Conversion between the number of molecules N of FFS experiments and the concentration [A] is accomplished by $[A] = N/V_{PSF}$ (where PSF is the point spread function). The value of the PSF volume V_{PSF} is calibrated from a measurement of a dye solution of known concentration (1). In the absence of FRET, the fluorescence intensities in the red and green channel are given by

$$\langle F_{\mathbf{R}} \rangle = \lambda_{\mathbf{R},D} N_{D_t} + \lambda_{\mathbf{R},A} N_{A_t}, \quad \langle F_{\mathbf{G}} \rangle = \lambda_{\mathbf{G},D} N_{D_t} \qquad \textbf{[S1]}$$

where $[D_t] = N_{D_t}/V_{\mathrm{PSF}}$ and $[A_t] = N_{A_t}/V_{\mathrm{PSF}}$ represent the total concentration of EGFP and mCherry fluorophores of the sample. The total concentration of mCherry is thus determined as

$$[A_t] = \frac{\langle F_{\mathbf{R}} \rangle - \langle F_{\mathbf{G}} \rangle \lambda_{\mathbf{R},D}/\lambda_{\mathbf{G},D}}{V_{\mathrm{PSF}} \lambda_{\mathbf{R},A}}. \qquad \textbf{[S2]}$$

Because $\lambda_{\mathbf{R},D} < \lambda_{\mathbf{R},A}$ and $[D_t] < [A_t]$ in our experimental conditions, we often approximate Eq. **S2** by $[A_t] = \langle F_{\mathbf{R}} \rangle / (V_{\mathrm{PSF}} \lambda_{\mathbf{R},A})$.

The experiments are performed on cells with a protein concentration ratio r_{AD}=$r_{AD} = [A_t]/[D_t]$ exceeding a preset value. Such cells are conveniently identified from the fluorescence intensity ratio r_F of the detection channels,

$$r_F = \frac{\langle I_{\mathbf{R}} \rangle}{\langle I_G \rangle} \geq \frac{r_{AD} \lambda_{\mathbf{R},A} + \lambda_{\mathbf{R},D}}{\lambda_{\mathbf{G},D}}. \qquad \textbf{[S3]}$$

Only cells that fulfill the condition of Eq. **S3** are selected for FFS measurements. The equations have been derived assuming no FRET, which is sufficient to describe the experiments described in this paper. The presence of FRET leads to changes in the above equations as described elsewhere (4).

FFS measurements are performed by focusing the laser at the cell's midsection in the vicinity of the center of the nucleus, while avoiding nucleoli. To check the repeatability of the FFS experiments, we performed a second FFS experiment in the same cell after moving the laser focus laterally by 1–2 μm. This study was carried out on 10 cells before and after adding the ligand 9-*cis* retinoic acid. The two measurements agreed with one another to within a standard deviation of ∼20%.

Additional HSP Modeling. ***Brightness titration for a two-state model of A*** The main text describes the heterospecies model for A existing in a single brightness state. Here we develop the heterospecies model for A existing in two brightness states to reflect experiments performed with mCherry as protein A. All modeling will be based on parameters determined for mCherry for excitation at 1,000 nm (3). The two states of mCherry are referred to as A(1) and A(2). The population fraction of state 1 is $\alpha = 0.23$ and the brightness ratio between both states is $\theta = \lambda_{\mathbf{R},\mathrm{A}(2)}/\lambda_{\mathbf{R},\mathrm{A}(1)} = 0.29$. Modeling will use the following brightness values for A

(x) and D: $\lambda_{\mathbf{G},D} = 1260$ cps, $\lambda_{\mathrm{R},D} = 90$ cps, $\lambda_{\mathbf{R},\mathrm{A}(1)} = 1.54\tilde{\lambda}_{\mathbf{R},\mathrm{A}}$, and $\lambda_{\mathbf{R},\mathrm{A}(2)} = 0.45\lambda_{\mathbf{R},\mathrm{A}}$, where $\lambda_{\mathbf{R},A} = 360$ cps is the average brightness of the A existing as a mixture of two states. All modeling is performed assuming no FRET between D and A. Details about modeling brightness analysis of mCherry in the presence of FRET can be found elsewhere (3).

Cumulants accounting for the two states of A are constructed by summing up the cumulants of each of the two states,

$$\kappa^{\{A\}}_{[i,j]} = \gamma_{i+j} N T^{i+j} (\alpha \lambda^i_{\mathbf{R},\mathrm{A}(1)} 0^j + (1-\alpha)\lambda^i_{\mathbf{R},\mathrm{A}(2)} 0^j). \quad \textbf{[S4]}$$

Similarly, the cumulants accounting for the two states of DA are (2, 3)

$$\kappa^{\{DA\}}_{[i,j]} = \gamma_{i+j} N T^{i+j} (\alpha \lambda^i_{\mathbf{R},\mathrm{DA}(1)} \lambda^j_{\mathbf{G},\mathrm{DA}(1)} + (1-\alpha)\lambda^i_{\mathbf{R},\mathrm{DA}(2)} \lambda^j_{\mathbf{G},\mathrm{DA}(2)}), \quad \textbf{[S5]}$$

where

$$\lambda_{\mathbf{R},\mathrm{DA}(x)} = \lambda_{\mathbf{R},\mathrm{D}} + \lambda_{\mathbf{R},\mathrm{A}(x)}, \quad \lambda_{\mathbf{G},\mathrm{DA}(x)} = \lambda_{\mathbf{G},\mathrm{D}} \quad \textbf{[S6]}$$

describes the brightness of heterodimer states DA(1) and DA(2). The cumulants of the heterodimer equilibrium are determined by summing the cumulants of each species present,

$$\kappa_{[i,j]} = \kappa^{\{A\}}_{[i,j]} + \kappa^{\{D\}}_{[i,j]} + \kappa^{\{DA\}}_{[i,j]} \quad \textbf{[S7]}$$

The brightness vector of the heterospecies H is determined by fitting Eq. S7 to Eq. 1 of the main text.

Next, we determine the brightness titration curve for the heterodimer reaction $\mathrm{D} + \mathrm{A} \leftrightarrow \mathrm{DA}$. The red-channel brightness $\lambda_{\mathbf{R},H}$ is determined using the two-state model of A for expression ratios of 10 and 2. The brightness $\lambda_{\mathbf{R},H}$ is converted into the degree of binding y by normalization of the brightness titration curve, $y = (\lambda_{\mathbf{R},H} - \lambda_{\mathbf{R},D})/(\lambda_{\mathbf{R},DA} - \lambda_{\mathbf{R},D})$. Fig. S1 shows the titration curves for both the two-state model and the one-state model of A for identical protein expression ratios. The figure demonstrates that in the absence of FRET the two-state model of A leads to the same results as the single-state model discussed in the main text.

In addition, we explore the behavior of the titration curves for $\mathrm{D} + 2\mathrm{A} \leftrightarrow \mathrm{DA}_2$ with A existing in two brightness states. Modeling proceeds as outlined in Eqs. **S4**–**S7**, while accounting for the presence of the heterotrimer DA_2. The equations describing the cumulants of each of the four possible brightness states of the heterotrimer are available (3). The red-channel brightness $\lambda_{\mathbf{R},H}$of the heterospecies is determined by a fit of the cumulants as described earlier. The brightness is converted into a generalized degree of binding by $y = 2(\lambda_{\mathbf{R},H} - \lambda_{\mathbf{R},D})/(\lambda_{\mathbf{R},DA_2} - \lambda_{\mathbf{R},D})$. Fig. S2 shows the binding curves for the two-state model and the one-state model of A for expression ratios of 20 and 4. The figure illustrates that both models lead to virtually identical binding curves.

Brightness titration of $D + A \leftrightarrow DA$ in the presence of FRET. We consider the influence of FRET between the donor D and the acceptor A on titration experiments. The brightness vector of the heterodimer in the presence of FRET with efficiency E is given by (4, 5)

$$\begin{aligned}\vec{\lambda}_{DA} &= (\lambda_{\mathbf{G},DA}, \lambda_{\mathbf{R},DA}) \\ &= (\lambda_{\mathbf{G},D}(1-E), \lambda_{\mathbf{R},D}(1-E) + \lambda_{\mathbf{R},A}(1+\sigma_r E)), \end{aligned} \quad \textbf{[S8]}$$

where σ_r is the ratio of the absorption cross-section between D and A (44). The cumulants for the reaction $\mathrm{D} + \mathrm{A} \leftrightarrow \mathrm{DA}$ are calculated as in the main text,

$$\kappa_{[i,j]} = \gamma_{i+j} T^{i+j} (\lambda^i_{\mathbf{G},D} \lambda^j_{\mathbf{R},D} N_D + 0^i \lambda^j_{\mathbf{R},A} N_A + \lambda^i_{\mathbf{G},DA} \lambda^j_{\mathbf{R},DA} N_{DA}) \quad \textbf{[S9]}$$

except that the brightness of the heterodimer DA is now described by Eq. **S8**. Fitting of these cumulants to the HSP model determines the brightness vector of the heterospecies. Brightness titration curves are determined for given r_{AD}, $\vec{\lambda}_D$, $\vec{\lambda}_A$, σ_r, and E, while varying the degree of binding y. The titration curves are normalized by

$$\hat{y} = \frac{\lambda_{\mathbf{R},H} - \lambda_{\mathbf{R},D}}{\lambda_{\mathbf{R},DA} - \lambda_{\mathbf{R},D}}, \quad \textbf{[S10]}$$

where $\hat{y}$ represents the experimentally measurable degree of binding in the presence of FRET. Modeling reveals that the normalized binding curves are independent of the values chosen for $\vec{\lambda}_D$, $\vec{\lambda}_A$, and σ_r. However, the brightness titration curves shift to higher concentrations as the FRET efficiency E increases (Fig. S3). Thus, the experimentally measured $\hat{y}$ represents a biased value for the degree of binding y in the presence of FRET. The brightness titration curve only represents the true binding curve in the absence of FRET ($E = 0$). However, it is straightforward to correct the shift in the brightness titration curve from the experimentally determined FRET efficiency. Fig. S3 shows that the shift in the binding curve is less than a factor of 1.5 for FRET efficiencies $E < 30\%$. Thus, given the typical experimental uncertainty of brightness measurements in cells, the shift in the brightness titration curve is to first-order negligible. Because we observed FRET efficiencies of less than 30% for direct fusion proteins between EGFP and mCherry (3), we expect that most interactions between proteins using these labels result in FRET efficiencies that are <30%. Thus, it appears that HSP analysis provides a fairly robust measure of protein–protein heterointeraction in cells.

Control Experiments. ***Oligomeric state of TIF-2.*** In a separate experiment, cells transfected with EGFP-TIF-2 were measured to verify that the coactivator is not forming homocomplexes as required by the HSP analysis method. The normalized brightness, defined as the brightness of EGFP-TIF-2 divided by the brightness of EGFP, is according to Fig. S4 close to one as a function of protein concentration. This result demonstrates the absence of homocomplex formation of the coactivator.

TIF-2. The coactivator TIF-2 is probed by Western blotting using TIF-2-antibody (Fig. S5*A*). The first lane shows the blot for CV-1 cells expressing EGFP. A single faint band representing endogenous TIF-2 is present. The second lane probes cells expressing EGFP-labeled TIF-2. Two bands representing endogenous TIF-2 and exogenous EGFP-TIF-2 are detected. Quantification of the integrated band intensities implies >20-fold excess of the exogenous over the endogenous protein. Considering that only 10–20% of cells are transfected, the concentration of unlabeled, endogenous TIF-2 protein is, on average, at most 1% of the labeled, exogenous TIF-2. Thus, the endogenous concentration of most cells expressing EGFP-TIF-2 is negligible.

We further probed cells expressing EGFP-TIF-2 by Western blotting using a GFP antibody (Fig. S5*B*). A faint band representing EGFP-TIF-2 is detected. No other bands that would indicate cleaved EGFP-TIF-2 are detected. For comparison, the gel also depicts a blot for the protein EGFP. Together these data indicate that EGFP-TIF-2 is expressed as a full-length protein together with a very small concentration of endogenous TIF-2.

RXR and RXRLBD. The ligand binding domain of RXR is at the C terminus. A ligand induced conformational change of helix 12 is crucial for RXR interaction with coactivators and corepressors (6). Therefore it is favorable to label nuclear receptors at the N terminus instead of the C terminus. However, N-terminal

labeling could lead to fluorescence even if RXR or RXRLBD is not fully expressed. To establish the expression of full-length protein, Western blots of EGFP-RXR (mCherry-RXRLBD and mCherry-RXR) expressing cells probed by GFP (DsRed) antibody are shown in Fig. S6. The blot depicts for each protein a single discrete band with the correct molecular weight, which establishes the expression of full-length protein. For comparison, the figure also shows a blot for EGFP expressing cells.

We previously demonstrated that the endogenous concentration of RXR in Cos-1 cells is negligible compared to the exogenously expressed protein (7). Because CV-1 and Cos-1 cells are closely related, we expect the same result to hold true in CV-1 cells. As a check we compared the brightness binding curve of RXRLBD in both cell lines. If endogenous protein is negligible, we expect the same binding curve for both cell lines, as is experimentally observed (Fig. S7).

1. Wu B, Müller JD (2005) Time-integrated fluorescence cumulant analysis in fluorescence fluctuation spectroscopy. *Biophys J* 89:2721–2735.
2. Wu B, Chen Y, Müller JD (2006) Dual-color time-integrated fluorescence cumulant analysis. *Biophys J* 91:2687–2698.
3. Wu B, Chen Y, Müller JD (2009) Fluorescence fluctuation spectroscopy of mCherry in living cells. *Biophys J* 96:2391–2404.
4. Chen Y, Wei LN, Müller JD (2005) Unraveling protein–protein interactions in living cells with fluorescence fluctuation brightness analysis. *Biophys J* 88:4366–4377.
5. Hillesheim LN, Chen Y, Müller JD (2006) Dual-color photon counting histogram analysis of mRFP1 and EGFP in living cells. *Biophys J* 91:4273–4284.
6. Egea PF, et al. (2000) Crystal structure of the human RXR[alpha] ligand-binding domain bound to its natural ligand: 9-*cis* retinoic acid. *EMBO J* 19:2592–2601.
7. Chen Y, Wei LN, Müller JD (2003) Probing protein oligomerization in living cells with fluorescence fluctuation spectroscopy. *Proc Natl Acad Sci USA* 100:15492–15497.

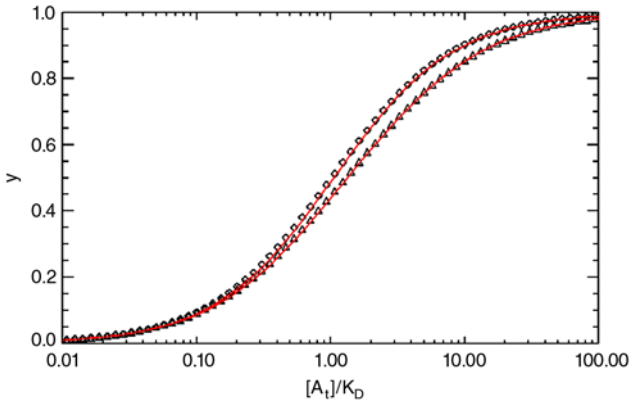

Fig. S1. Brightness titration plot for the case that protein A exists in two brightness states assuming a protein expression ratio of $r_{AD} = 10$ (◇) and $r_{AD} = 2$ (Δ). The curves are determined using the experimental brightness values of EGFP and mCherry. The red-channel brightness of the heterospecies is converted into the degree of binding *y* as described in the text. The two solid lines represent equivalent brightness titration curves determined for the case that A exists in a single brightness state.

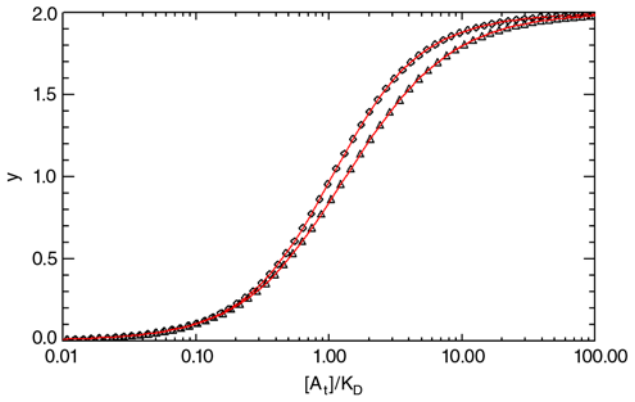

Fig. S2. Brightness titration plot for the heterotrimer reaction $D + 2A \leftrightarrow DA_2$. Titration curves are determined for expression ratios of $r_{AD} = 20$ (◇) and $r_{AD} = 4$ (Δ) using a two-state model for A with parameters that represent mCherry and EGFP. Both binding steps of the reaction are assumed to have the same K_D. The red-channel brightness of the heterospecies is converted into the degree of binding *y* as described in the text. The two solid lines represent binding curves determined for r_{AD} of 20 and 4 using a single-brightness state for A.

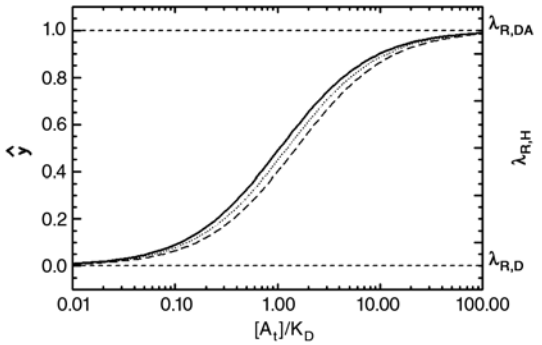

Fig. S3. Brightness titration plot for D + A ↔ DA in the presence of FRET for efficiencies of 0% (solid line), 15% (dotted line), and 30% (dashed line). The brightness titration curves are calculated for $r_{AD} = 10$ and normalized as described in the text. The parameter $\hat{y}$ represents an approximation of the true degree of binding y. Note that $\hat{y} = y$ in the absence of FRET (solid line). The presence of FRET leads to an apparent shift of the brightness titration curve to higher concentrations.

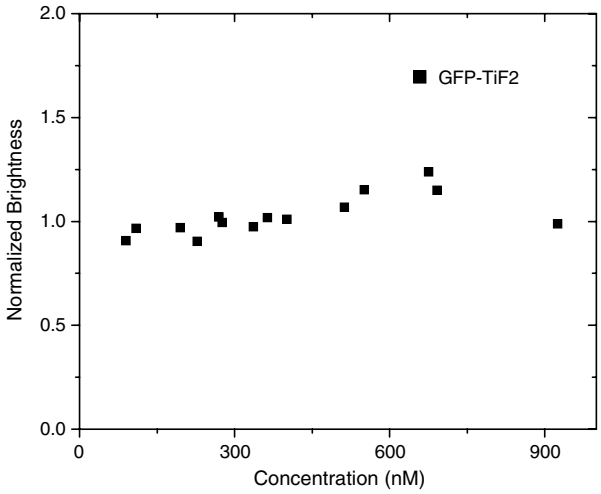

Fig. S4. Normalized brightness of EGFP-TIF-2 as a function of concentration. The normalized brightness stays close to one, which demonstrates the absence of homocomplex formation of EGFP-TIF-2 as required by the HSP model.

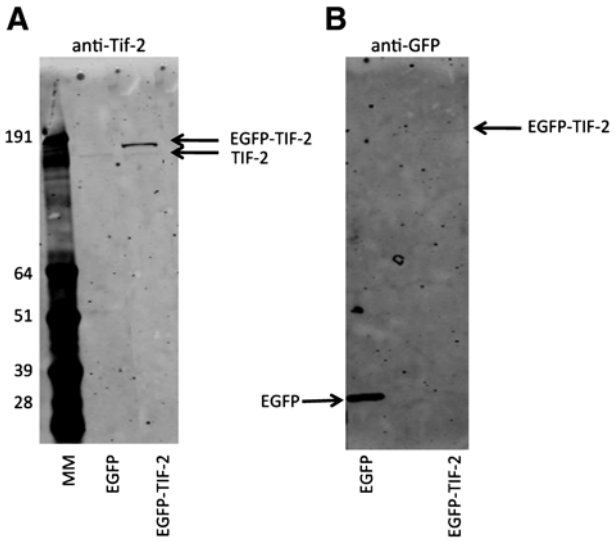

Fig. S5. Western blot analysis of Tif-2 in CV-1 cells. (*A*) M, molecular weight marker with sizes in kilodaltons indicated on the left; EGFP, cells transfected with EGFP and probed with anti-TIF-2 antibody; EGFP-TIF-2, cells transfected with EGFP-TIF-2 and probed with anti-TIF-2 antibody. (*B*) EGFP, cells transfected with EGFP and probed with anti-GFP antibody; EGFP-TIF-2, cells transfected with EGFP-TIF-2 and probed with anti-GFP antibody. The images are contrast enhanced to improve visibility of faint bands.

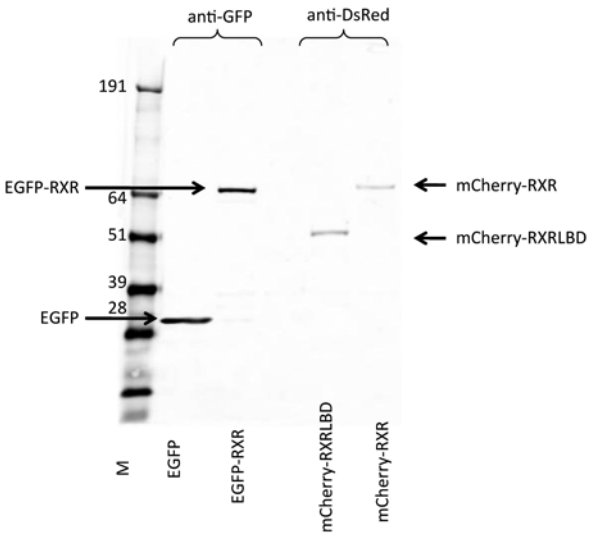

Fig. S6. Western blot analysis of RXR and RXRLBD in CV-1 cells. The label of each lane specifies the protein expressed by the transfected cells. EGFP is probed with an anti-GFP antibody, whereas mCherry is probed by an anti-DsRed antibody.

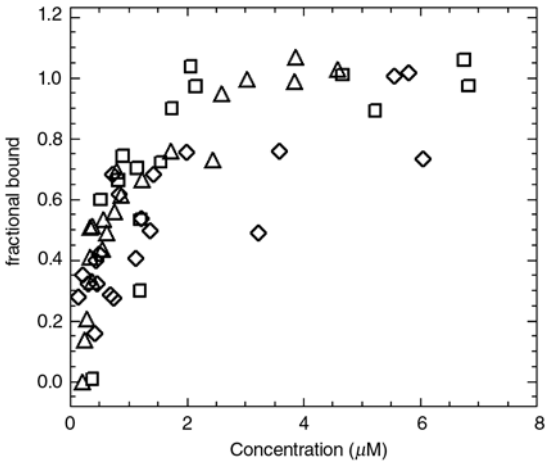

Fig. S7. Binding curve for labeled RXRLBD in the presence of 1 μM 9-*cis* retinoic acid. The experimentally measured brightness of EGFP-RXRLBD in CV-1 cells (Δ), mCherry-RXRLBD in CV-1 cells (□), and EGFP-RXRLBD in Cos-1 cells (◇) is converted into the bound fraction ($f = 2n_2/(n_1 + 2n_2)$, where n_1 and n_2 are the monomer and dimer concentration, respectively) and plotted as a function of protein concentration.